J. Coat. Technol. Res., **17** (5) 1217–1230, 2020
https://doi.org/10.1007/s11998-020-00341-4

Sustainable cardanol-based multifunctional carboxyl curing agents for epoxy coatings: Si–S synergism

Kunal Wazarkar, Anagha Sabnis

Abstract High-performance epoxy coatings were prepared by crosslinking commercial diglycidyl ether of bisphenol-A with silicon–sulfur containing di- and tetra-functional carboxyl curing agents based on cardanol. The curing agents were synthesized and products were analyzed by chemical, spectroscopic, and chromatographic techniques. In the next part, coatings were formulated by varying the ratio of epoxy resin to curing agents on equivalent basis, such as 1:0.6, 1:0.8, and 1:1. The coatings were applied on mild steel panels and cured at 150°C for 30 min. The resultant coatings were evaluated for performance properties including mechanical, chemical, optical, thermal anticorrosive, and flame retardant properties. It was observed that with an increase in concentration of silicon–sulfur containing curing agents, water contact angles of the coatings substantially increased. Moreover, electrochemical impedance spectroscopy, Tafel analysis, and salt spray studies revealed that anticorrosive properties of the coatings improved with an increase in concentration of silicon and sulfur. In spite of synergistic effect of silicon–sulfur, only marginal improvement in flame retardant properties was observed.

Electronic supplementary material The online version of this article (https://doi.org/10.1007/s11998-020-00341-4) contains supplementary material, which is available to authorized users.

K. Wazarkar, A. Sabnis (✉)
Department of Polymer and Surface Engineering, Institute of Chemical Technology, Matunga, Mumbai 400019, India
e-mail: as.sabnis@ictmumbai.edu.in

Graphic abstract

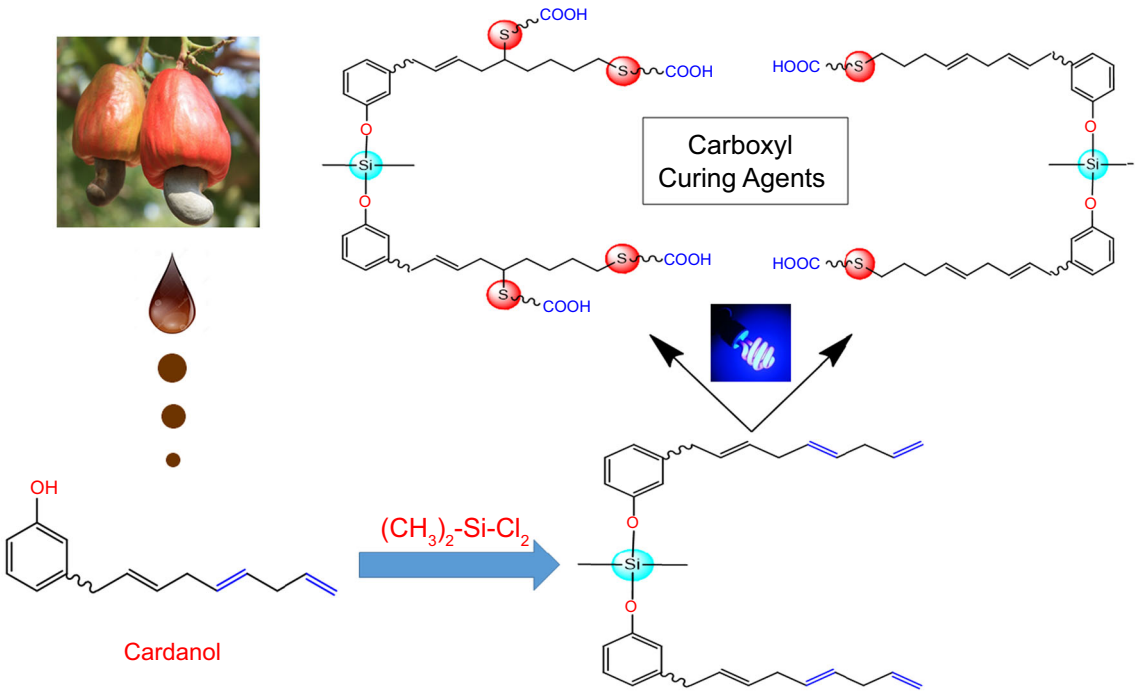

Keywords Cardanol, Hydrophobic, Anticorrosive, Synergistic, Silicon–sulfur

Introduction

Epoxy resins with a unique combination of properties have occupied a dominant place in the development of high-performance materials.[1,2] At the same time, more demanding requirements of the end users for higher thermal stability and greater resistance to oxidation of these materials push the existing technology and knowledge to their limits. Such challenging requirements have forced researchers to develop a new class of organic–inorganic hybrid polymers.

In recent years, owing to their low surface energy, superior thermal stability, excellent moisture resistance, and hydrophobicity, silicone compounds are considered to be among the best modifiers for epoxy resins.[3] Moreover, research revealed that the addition of small amounts of silicon compounds to various polymeric materials has a flame retardant effect. Silicon-containing compounds are recognized as another kind of environmentally friendly flame retardant because of their reduction in the harmful impact on the environment.[4,5] This is partly because these compounds dilute the concentration of flammable species and partly because the siliceous residues can form a barrier to an advancing flame.[6–9] Moreover, silicon-containing compounds can migrate to the surface of a polymer substrate at high temperature due to their low surface energy. The high silicon concentration on the surface further improves the flame retardancy of compounds.[10–12] However, the flame retardant efficiency of single silicon-containing compounds is not high enough and cannot meet the requirement of polymer materials.[13–15] Therefore, they are often blended with other compounds containing phosphorus, nitrogen, sulfur, etc., which synergistically improves the flame retardancy of the polymer systems to which they are added.[16–19] For example, Chao et al.,[20] synthesized two novel phosphorus–silicon–nitrogen containing flame retardants bearing active hydroxyl group to improve compatibility with epoxy matrix. Results revealed that addition of 15 wt% flame retardants increased limiting oxygen index (LOI) values from 20 to 27 as well as resulted in improvement in thermal stability. Similarly, Zhang et al.,[21] developed epoxy composites incorporated with a phosphorus–silicon–nitrogen compound and observed that the best formulation exhibited an LOI value as high as 34 and V-0 rating on UL-94 test. In a more recent work, graphene oxide modified with a phosphorus–nitrogen–silicon compound was used as a flame retardant for epoxy resins. The authors concluded that resultant composites exhibited excellent mechanical, thermal, and flame retardant properties.[22]

Although these compounds are efficient flame retardants, they are based on petroleum resources. In recent years, depletion of fossil fuels as well as

stringent environmental regulations has forced researchers to develop sustainable products that are derived from renewable resources. Among various renewable resources, cardanol is one such compound that is obtained from cashew nut shell liquid (CNSL), which is inexpensive and abundantly available in all parts of world.[23,24] Cardanol has a phenolic hydroxyl group and a meta-substituted long alkyl chain. This unique structure allows easy chemical modification via a number of reaction chemistries to obtain products with balanced performance properties. Today, cardanol and its derivatives are widely used in the preparation of coatings, curing agents, surfactants, adhesives, antioxidants, etc.[25–30]

In our previous work, we synthesized silicon-containing anhydride curing agent for epoxies, and it was observed that silicon played an important role in obtaining excellent performance properties for the coatings.[31] In a similar manner, we have attempted to synthesize cardanol-based silicon–sulfur containing multifunctional carboxyl curing agents for high-performance epoxy coatings.

Materials

Cardanol (NC-700) was kindly provided by Cardolite Specialty Chemicals Ltd., Mangalore, India. Commercial epoxy resin (diglycidyl ether of bisphenol-A; % solids—70 and EEW—180/eq) was procured from Huntsman India Ltd., Mumbai, India. All the reagent grade chemicals, including dichlorodimethylsilane (DCDMS), thioglycolic acid, *N*,*N*-dimethylbenzylamine (BDMA), 1,8-diazabicycloundec-7-ene (DBU), Irgacure-184, sodium hydride, sodium hydroxide, butanol, tetrahydrofuran, ethyl acetate, and xylene, were purchased from SD Fine Chemicals, Mumbai, India. All reagent grade chemicals were used as received without further purification.

Experimental

Synthesis of silicon containing dimer of cardanol (SIL)

The product SIL was synthesized as per method described in our previous work.[31] In the first step, 100 mL of ethyl acetate was poured into the four-necked flask fitted with water condenser, thermometer pocket, nitrogen inlet, and dropping funnel. The entire assembly was put into an ice bath, and stoichiometric amount of sodium hydride was added into the flask slowly. After that, cardanol was added to the above mixture in a dropwise manner for a period of 20–25 min by maintaining the temperature maximum at 10°C. After complete addition of cardanol, the temperature of the mixture was gradually increased to 60–70°C, and the mixture was allowed to stir for one hour. Further, the reaction mixture was again cooled to 5–10°C, and dichlorodimethylsilane was added dropwise for a period of 1–1.5 h. The stoichiometric ratio of cardanol/DCDMS/sodium hydride was 2:1:2. After complete addition of DCDMS, the temperature of the mixture was gradually raised to 70°C and allowed to stir for 8 h. The product, abbreviated as SIL, was then washed several times with lukewarm water to ensure complete removal of sodium chloride salt.

Synthesis of Si–S containing multifunctional carboxyl curing agents

Thiol-ene coupling of SIL was performed in a single-necked round-bottom flask fitted with water condenser and placed on a magnetic stirrer. To obtain di- and tetra-functional carboxyl curing agents, the molar ratio of SIL to thioglycolic acid was varied as 1:6 and 1:10, respectively. The reaction mixture consisted of stoichiometric amount of SIL and thioglycolic acid along with 1 wt% (of total solids) photoinitiator Irgacure-184 and 1.5 wt% (of total solids) DBU catalyst. The reaction mixture was allowed to reflux at 80°C for 20 h in the presence of UV light. After completion of the reaction, the mixture was diluted in ethyl acetate and washed several times with 1% aq. sodium hydroxide solution followed by washings with lukewarm water to ensure complete removal of unreacted compounds. The organic layer was then separated and evaporated to obtain di- and tetra-functional curing agents, which were abbreviated as S-I and S-II, respectively. The structure of curing agents was analyzed with chemical and spectroscopic analysis (as shown in Fig. 1).

Formulation of coatings

The synthesized curing agents were mixed with commercial epoxy resin in varying proportions as 1:0.6, 1:0.8, and 1:1 (see Table 1). The calculated amount of epoxy adduct and carboxyl curing agents along with 1 wt% (of total solids) BDMA was mixed with xylene/butanol (70/30 on v/v) to attain application viscosity. The coating mixture was applied on mild steel panels, and, after a flash-off time of 10 min, coated substrates were kept in an air circulating oven. The panels were thermally cured at 150°C for 30 min to achieve complete cure. After 24 h of conditioning, the coated panels were evaluated for physical, mechanical, chemical, thermal, anticorrosive, and flame retardant properties. Coatings cured with 0.6, 0.8, and 1 equivalent of S-I and S-II were represented by the name of curing agent followed by numbers 0.6, 0.8, and 1, respectively. The amount of curing agent required for curing epoxy resin is given by equation (1)

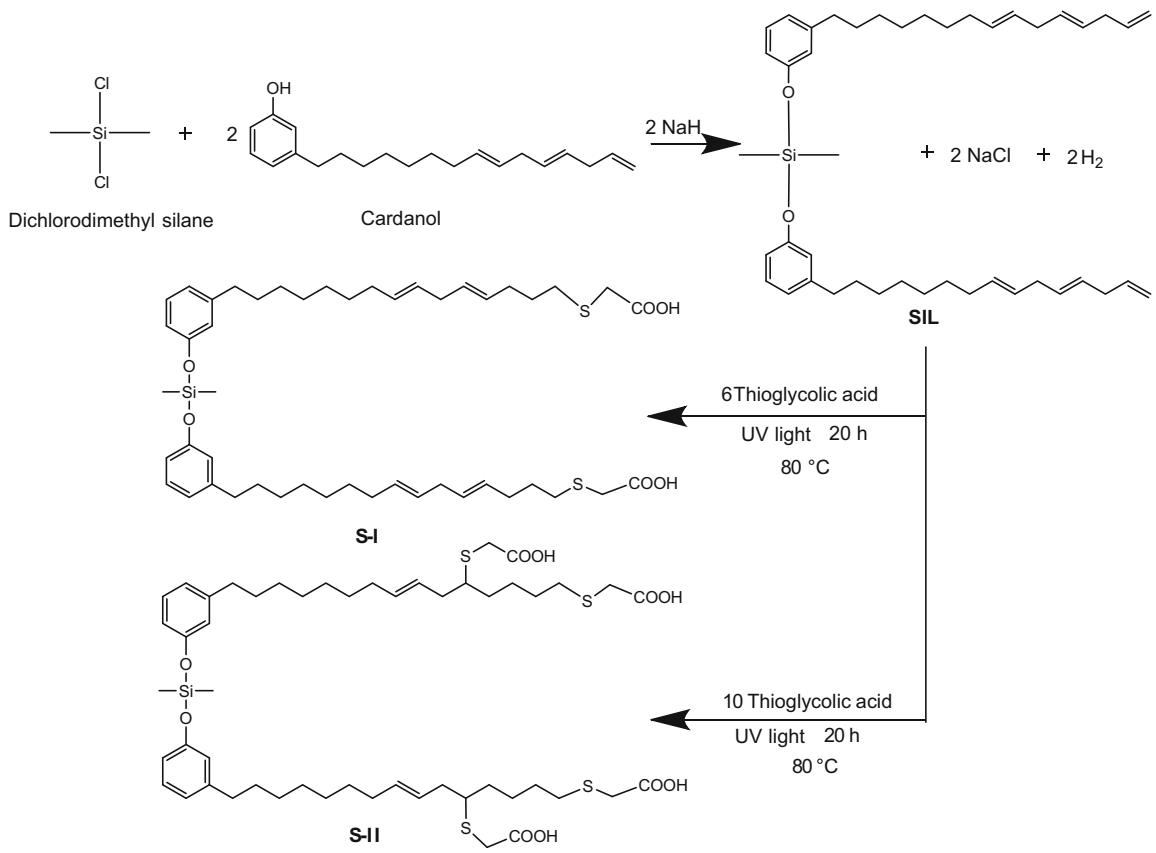

Fig. 1: Schematic representation of preparation of Si–S containing multifunctional curing agents

Table 1: Formulation of epoxy coatings

Coating	Qty required per 100 g epoxy	Silicon (wt%)	Sulfur (wt%)
S-I-0.6	141.4	1.93	4.42
S-I-0.8	188.5	2.16	4.93
S-I-1.0	235.6	2.32	5.29
S-II-0.6	86	1.25	5.73
S-II-0.8	114.7	1.45	6.62
S-II-1.0	143.4	1.6	7.30

$$\frac{\text{Weight of epoxy}}{\text{Epoxy equivalent weight}} = \frac{\text{Weight of curing agent}}{\text{No. of equivalents} \times \text{equivalent weight of curing agent}} \quad (1)$$

Characterization

The acid and iodine values were evaluated as described in ASTM D1980 and ASTM D1959, respectively. To calculate gel content (GC), known weight of sample ($W0$) was put into 20 mL tetrahydrofuran for 24 h. After completion of test period, the solution was filtered and contents of filter paper were dried in an oven at 50°C and weighed again ($W1$). GC was then calculated using equation (2).

$$\text{Gel content } (\%) = \frac{W1 * 100}{W0} \quad (2)$$

To measure water absorption of coating films, a sample with known weight was kept in water at room temperature for 24 h. After completion of the test period, any drops of water left on film samples were soaked with cotton and sample was weighed. The

water absorption was calculated according to equation (3)

$$\text{Water absorption } (\%) = \frac{(W_{\text{after}} - W_{\text{before}}) \times 100}{W_{\text{before}}} \quad (3)$$

where W_{after} is the weight of the sample after dipping in water, and W_{before} is the weight of the sample before dipping in water.

Dry film thickness of all the coatings was measured by using DFT meter. DFT meter was calibrated using zero calibration method and standard calibration foils of 25, 50, 75, and 200 microns. The adhesion of the coatings was evaluated by cross-cut adhesion according to ASTM D3359. A lattice pattern of cuts with equal spacing was made on the coating surface with the crosshatch cutter, and commercial cellophane tape was applied over the lattice. The substrate was then examined for any loss of the squares from the lattice pattern. Gloss of the coatings was measured at 60° by gloss meter as per ASTM D523. Pencil and scratch hardness of the coatings were measured on hardness tester according to ASTM D3363 and IS-104, respectively. Flexibility of the coating films was examined by conical mandrel as per ASTM D522, and impact resistance was measured on impact tester with maximum height of 23.6 in and a load of 3 lbs as described in ASTM D2794. The chemical resistance of the coated panels was evaluated by acid and alkali immersion method according to ASTM D1308. Coated panels were inspected for degree of adhesion, visual inspection of blister, and cracks after immersion for 24 h. The solvent resistance was measured by solvent double rub test using methyl ethyl ketone and xylene as per ASTM D4752. Hydrolytic stability was evaluated according to ASTM B1308, and coated panels were immersed in boiling water for 4 h and examined for loss of adhesion and blister formation, if any.

Instrumentation

The FTIR spectra of curing agents were recorded on a Bruker instrument in the wavelength range of 4000–400 cm^{-1} with 24 scans and 2 cm^{-1} of resolution. NMR spectra of curing agents were recorded on Mercury Plus NMR spectrometer (400 MHz, Varian, USA). $CDCl_3$ was used as a solvent for all the samples. The chemical shifts in the discussion are reported in parts per million. The number average molecular weight (Mn) and molecular weight distribution was determined by gel permeation chromatography (GPC) (Agilent 1100 series). The sample was dissolved in tetrahydrofuran and placed in Agilent 1100 series instrument, consisting of a refractive index (RI) detector and Agilent PL gel 10 μm column. The thermogravimetric analysis (TGA) of coating films was performed on TGA Q-500 (TA Instruments, USA) under nitrogen atmosphere in the temperature range of 40–600°C at a heating rate of 10°C/min. Limiting oxygen index (LOI) was measured on alpha limiting oxygen chamber (Model no. 230) and minimum concentration of oxygen in a flowing mixture of oxygen and nitrogen that was just sufficient for flaming combustion was measured according to ASTM D2863. For this purpose, films were cast into Teflon mold and cut into dimensions of 80 mm × 50 mm × 0.2 mm. Samples were tested as per UL-94 vertical burning test according to ASTM D4804 on samples having 150 mm × 50 mm × 0.2 mm dimensions. Corrosion resistance of the coatings was evaluated by salt spray test, electrochemical impedance spectroscopy (EIS), and Tafel analysis. For this purpose, VersaSTAT-3 instrument (AMETEK, Princeton Applied Research, Oak Ridge, TN) was used, and all electrochemical measurements were obtained at room temperature (30°C) in 3.5% NaCl solution. The test system consisted of three electrode cells, in which calomel electrode, a platinum electrode, and a coated panel were used as reference, counter, and working electrodes, respectively. The area of the coated panels exposed to the NaCl solution was 7 cm^2 in all the cases. Salt spray test was conducted in salt spray chamber containing 5% NaCl solution as per ASTM B117, and panels were examined for creepage from scribe mark and % area failed according to ASTM D1654.

For DC polarization tests, corrosion rate of coatings was calculated using equation (4).[27]

$$\text{Corrosion rate (in mm/yr)} = \frac{3.27 \times I_{\text{corr}} \times E_{\text{w}}}{D \times A} \quad (4)$$

where I_{corr}—corrosion current density (mA); E_{w}—equivalent weight of steel = 27.6; D—density of steel = 7.86 g/cm^3; A—area of specimen = 7 cm^2.

All the experiments were conducted in duplicates to ensure the repeatability and consistency of the results.

Results and discussion

The synthesized curing agents S-I and S-II were analyzed by FTIR, ^{1}H-NMR, and ^{13}C-NMR spectroscopy for structural confirmation. Chemical analysis of products is shown in Table 2. As can be seen, theoretical acid and iodine values of products are very close to the experimental values confirming the desired product formation.

FTIR spectroscopy

Functional group analysis of both curing agents was done by FTIR spectroscopy. Figures S1 and S2 (see Supplementary Information) show the FTIR spectra of S-I and S-II, respectively. Addition of thioglycolic acid across the unsaturation of SIL was confirmed by the presence of the peak at 1709 cm^{-1} due to the –C=O

Table 2: Chemical analysis of Si–S containing carboxyl curing agents

Product	Acid value (mg of KOH/g)		Iodine value (g of I_2/100 g)	
	Theoretical	Practical	Theoretical	Practical
Cardanol	–	8.2	251.3	235.2
S-I	132.3	127.4	104.2	102.1
S-II	217.4	214.4	36.4	42.9

group and generation of –OH group which can be observed at 3363–3390 cm^{-1}. Other common peaks related to the methylene and methyl groups were observed at 2854 and 2921 cm^{-1}, respectively. Further, peaks at 1149–1151 cm^{-1} and 1263 cm^{-1} indicated the presence of Si–O–C and Si–C linkages in S-I and S-II.

^{1}H-NMR spectroscopy

^{1}H-NMR spectroscopy was performed to analyze chemical structure of S-I and S-II. Figures S3 and S4 (see Supplementary Information) show the NMR spectra of S-I and S-II, respectively. In both spectra, the chemical shift at 11 ppm could be assigned to the protons from –COOH group. Chemical shifts at 7.01–6.85 ppm could be attributed to the protons present in the aromatic ring. Methylene protons present in the aliphatic chain of cardanol could be observed at 1.29 ppm. To further confirm chemical structure of the curing agents, ^{13}C-NMR spectroscopy was performed, and spectra are shown in Supplementary Figs. S5 and S6. As shown in both figures, shifts at 172–176 ppm indicated the presence of carbon of –C=O group. Unsaturated carbon atoms present in the long chain of cardanol were observed at 129–130 ppm. Also, carbon atoms associated with aromatic ring could be observed at 112 and 156 ppm. So, it can be concluded that spectroscopic analyses of the products successfully confirm their chemical structure.

Gel permeation chromatography

Molecular weight of both the curing agents was determined by gel permeation chromatography, and curves are shown in Fig. 2. As shown in Table 3, practical molecular weights of curing agents were close to the theoretical molecular weights, confirming the formation of desired products.

Coating properties

Coating properties vary with chemical structure of curing agent, molecular weight, reactive functionality, and its concentration. In the present work, we have investigated the effect of varying concentration of

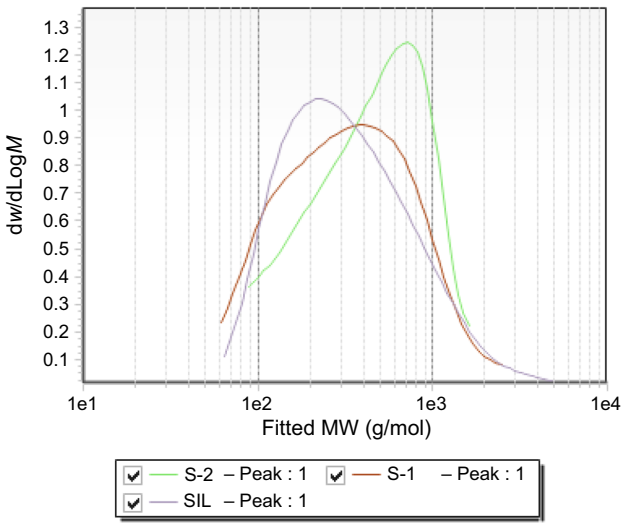

Fig. 2: GPC of products

Table 3: Molecular weight of products

Product	Theoretical Mol wt.	Practical Mol wt.	PDI
S-I	848	700	1.60
S-II	1032	947	1.54

curing agents on performance properties of coatings, and a structure property relationship was established.

Mechanical properties

All the coatings were applied on mild steel panels, and average dry film thickness was observed to be 50–60 microns. Coated panels were then analyzed for mechanical, chemical, thermal, anticorrosive, and flame retardant properties. Mechanical properties of coatings are summarized in Table 4. As can be seen, extent of crosslinking of all the coatings was observed to be excellent as less than 5% polymeric material dissolved in tetrahydrofuran even after 24 h. Moreover, irrespective of concentration of curing agent, all the coatings exhibited excellent adhesion to the mild steel substrate as indicated by 5B rating. Curing reaction of epoxy with acid curing agents resulted in the formation of secondary hydroxyl and polar car-

Table 4: Mechanical properties of coatings cured with S-I and S-II

Characterization	S-I-0.6	S-I-0.8	S-I-1.0	S-II-0.6	S-II-0.8	S-II-1.0
Gloss@60°	95 ± 5	100 ± 5	105 ± 5	97 ± 5	105 ± 5	115 ± 5
Gel content (%)	94.21	95.67	96.71	95.32	95.57	96.85
Adhesion	5B	5B	5B	5B	5B	5B
Pencil hardness	5H	6H	6H	6H	6H	6H
Scratch hardness (kg)	2.0	2.3	2.6	2.8	3.1	3.3
Impact resistance (lbs in)						
Intrusion	70.86	70.86	70.86	70.86	70.86	70.86
Extrusion	70.86	70.86	70.86	70.86	70.86	70.86
Flexibility (mm)	0	0	0	0	0	0
Water absorption (%)	1.25	0.86	0.62	1.14	0.74	0.56
Water contact angle (°)	89.16	91.33	93.44	96.85	97.64	98.22

bonyl ester groups. These polar groups attached with hydroxyl groups present on the metal substrate through secondary forces and were responsible for improving adhesion of coatings. Gloss of the coatings increased with an increase in concentration of curing agent, and coatings cured with S-II exhibited higher values of gloss than that of S-I counterpart. Two extra functionalities in S-II resulted in a highly crosslinked structure which may have been responsible for increasing gloss values. In a similar manner, coatings cured with S-II exhibited higher values of pencil hardness and scratch hardness than those of the coatings cured with S-I. Moreover, hardness improved with an increase in concentration of curing agents. Owing to the presence of four reactive carboxyl groups, coatings cured with S-II resulted in a more crosslinked and rigid polymer backbone as compared to the coatings cured with difunctional S-I. Similarly, increasing concentration of curing agents increased crosslinking in coating films and thus improved hardness of the coatings. Despite its four functionalities, coatings cured with S-II exhibited excellent flexibility and impact values. Furthermore, it was observed that irrespective of type and concentration of curing agents, all the coatings showed good load distribution properties. This could be attributed to the presence of two C15 aliphatic chains present in the structure of curing agents, which balanced the overall structure of coating and provided excellent flexibility and impact resistance values. Furthermore, water absorption studies revealed that coatings cured with S-I showed slightly higher values of water absorption. It was also observed that with increase in concentration of curing agent, % water absorption lowered. As explained earlier, four functionalities of S-II resulted in a more dense, hard, rigid, and compact structure than that of S-I, which subsequently reduced the passage of water through the coating and thus exhibited lower water absorption values. Water contact angle studies showed that with the increase in silicon content, hydrophobicity of coatings increased. In this case also, coatings cured with S-II showed higher water contact angle than those based on S-I (as shown in Fig. 3). The increase in water

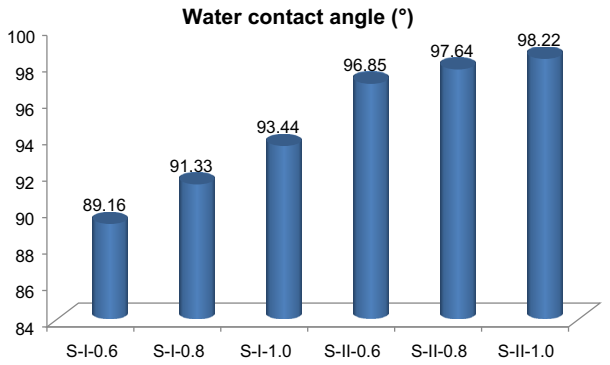

Fig. 3: Water contact angle of coated panels cured with S-I and S-II

contact angle could also be attributed to the presence of long aliphatic chains in the main backbone of S-I and S-II.

Chemical resistance

Chemical resistance of all the coated panels were evaluated by acid, alkali, and boiling water immersion method, and results are described in Table 5. For acid and alkali resistance, coated panels were dipped in the 5% aq. NaOH and 5% aq. HCl solutions for 24 h and inspected for any defect. It was observed that acid resistance of all the coatings was excellent as no loss of gloss, delamination, and blistering were observed on coated panels irrespective of type and concentration of curing agents. However, coatings dipped in alkaline solution showed slight loss of gloss due to the saponification of ester groups generated after curing reaction of epoxy with acid curing agents. In case of boiling water resistance, coated panels showed no visual defects even after 4 h of immersion, and all the coatings exhibited excellent hydrolytic stability. Resistance to solvents was evaluated by solvent double rub method. Regardless of the type of curing agent and its

Table 5: Chemical properties of coatings cured with S-I and S-II

Coating	Acid resistance	Alkali resistance	Hydrolytic stability	Solvent resistance	
				Xylene	MEK
S-I-0.6	No effect	Slight loss of gloss	No effect	> 200	> 200
S-I-0.8	No effect	Slight loss of gloss	No effect	> 200	> 200
S-I-1.0	No effect	Slight loss of gloss	No effect	> 200	> 200
S-II-0.6	No effect	Slight loss of gloss	No effect	> 200	> 200
S-II-0.8	No effect	Slight loss of gloss	No effect	> 200	> 200
S-II-1.0	No effect	Slight loss of gloss	No effect	> 200	> 200

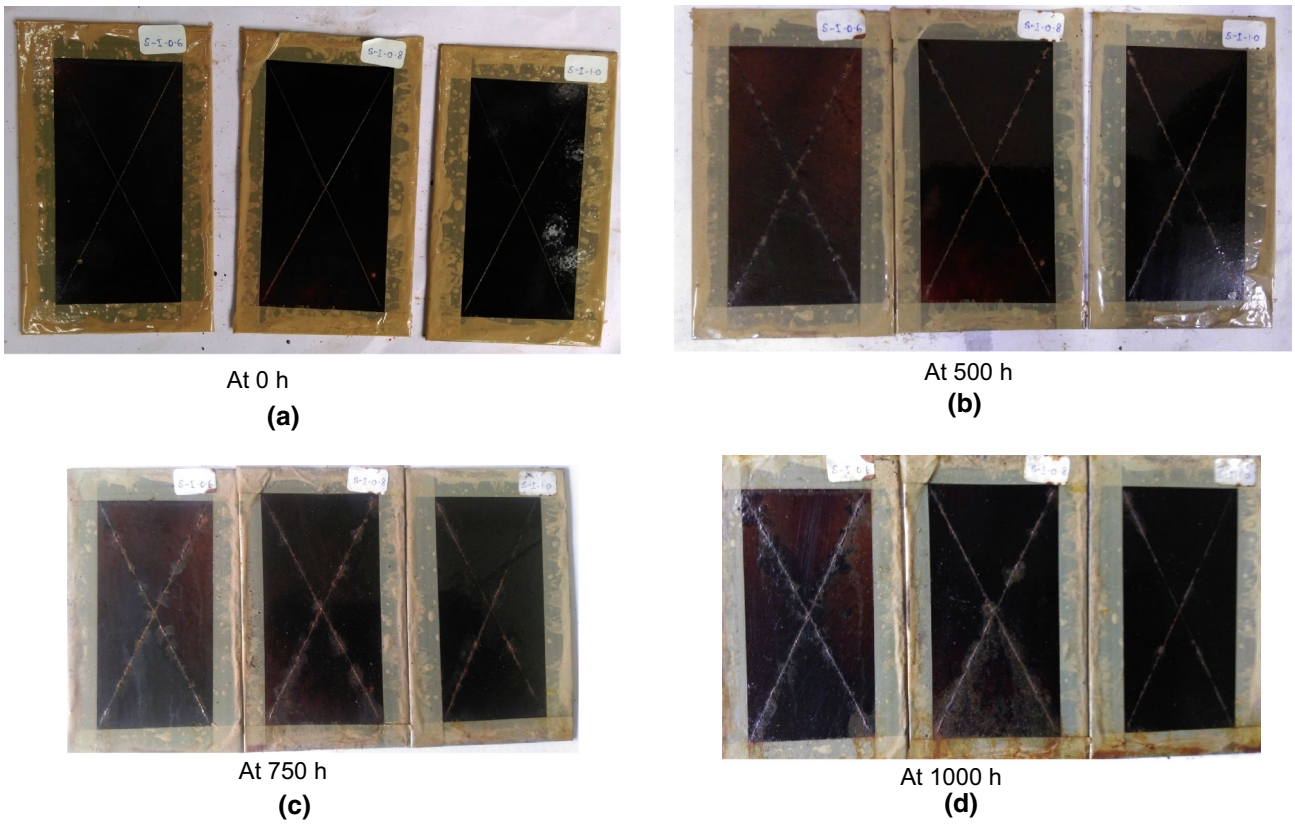

Fig. 4: Salt spray images of coated panels cured with S-I (a) at 0 h, (b) at 500 h, (c) at 750 h, (d) at 1000 h

concentration, resistance to xylene and methyl ethyl ketone for all the coatings was excellent as no loss of gloss, bleeding, blushing, etching, or dissolution of coating film was observed even after 200 rubs of each solvent.

Anticorrosive properties

Corrosion resistance of all the coatings was analyzed by salt spray test, Tafel analysis, and electrochemical impedance spectroscopy. The presence of silicon and sulfur affects barrier properties of the coatings. In addition, polar groups and the number of reactive functionalities also play important roles while evaluating the corrosion resistance.

SALT SPRAY TEST: Salt spray test was conducted in a salt spray chamber maintained at 35°C as per ASTM B117. All the coated panels were exposed to 5% aq. NaCl solution for 1000 h. Figures 4a–4d and 5a–5d show the salt spray images of coated panels before and after 0, 500, 750, and 1000 h of exposure. Table 6 represents the average creep values and % area failed of the coatings. For both S-I and S-II, no significant corrosion spread was observed even after 750 h.

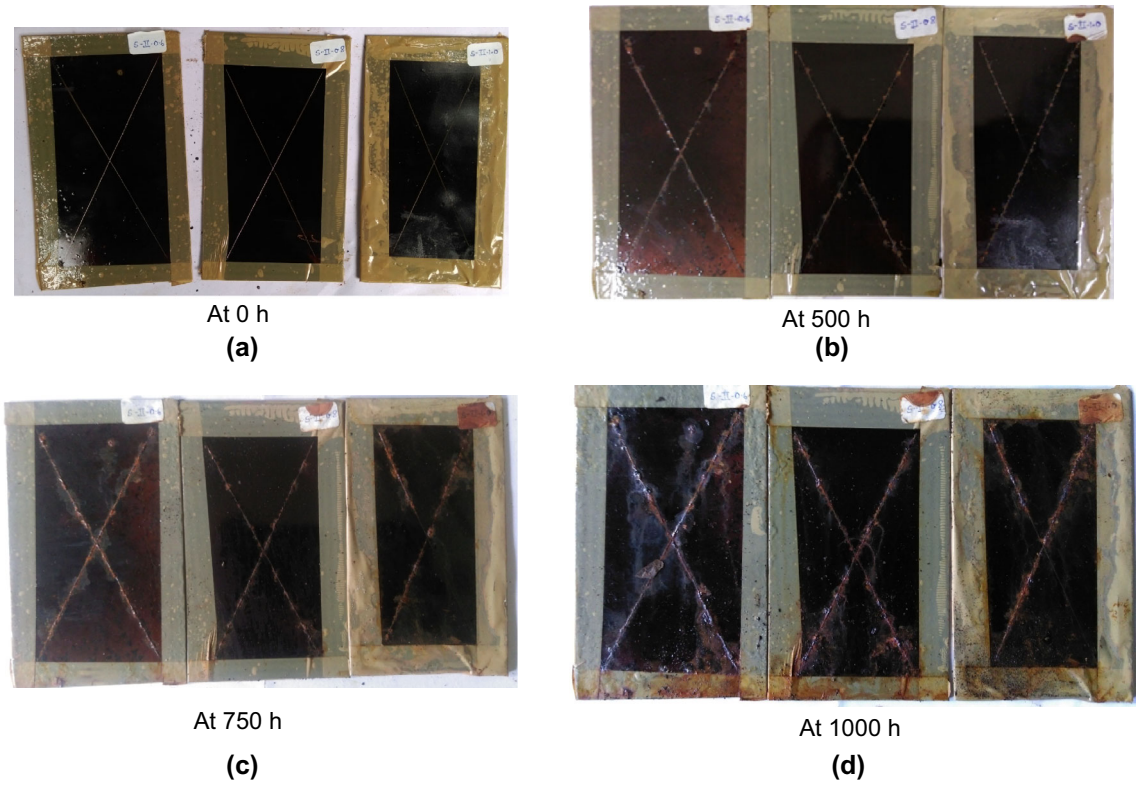

Fig. 5: Salt spray images of coated panels cured with S-II (a) at 0 h, (b) at 500 h, (c) at 750 h, (d) at 1000 h

Table 6: Average creep values and % area failed of the coatings

Coating	After 500 h		After 750 h		After 1000 h	
	Creep values	% area failed	Creep values	% area failed	Creep values	% area failed
S-I-0.6	8	9	6	7	5	5
S-I-0.8	9	10	7	8	6	4
S-I-1.0	9	10	8	9	7	8
S-II-0.6	9	9	6	6	4	5
S-II-0.8	10	10	8	9	5	5
S-II-1.0	10	10	8	8	7	6

Moreover, corrosion resistance improved with the increase in concentration of curing agents. Further, after completion of 1000 test hours, coatings cured with S-II exhibited slightly better resistance to corrosion than those based on S-I. This could be attributed to the higher concentration of sulfur and two additional functionalities present in S-II, which increased the barrier properties and improved corrosion resistance of the coatings. Nevertheless, in all the coatings, no delamination or etching of film was observed even after 1000 h of salt spray test, suggesting superior adhesion of coatings to the substrate. With increase in concentration of curing agents, effective concentration of silicon and sulfur increased, and at the same time, crosslink density of the coatings also increased. All these factors synergistically improved corrosion resistance of all the coatings.

ELECTROCHEMICAL IMPEDANCE SPECTROSCOPY: Quantitative measurement of the corrosion resistance was done by electrochemical impedance spectroscopy and is shown in Fig. 6. It was reported that organic compounds having two or more heteroatoms, such as sulfur, nitrogen, and oxygen, and multiple bonds in their molecular structure possess very good corrosion inhibition efficiency.[32–35] Moreover, these compounds exhibit a synergistic effect when added together to improve the anticorrosive properties significantly.[36] As

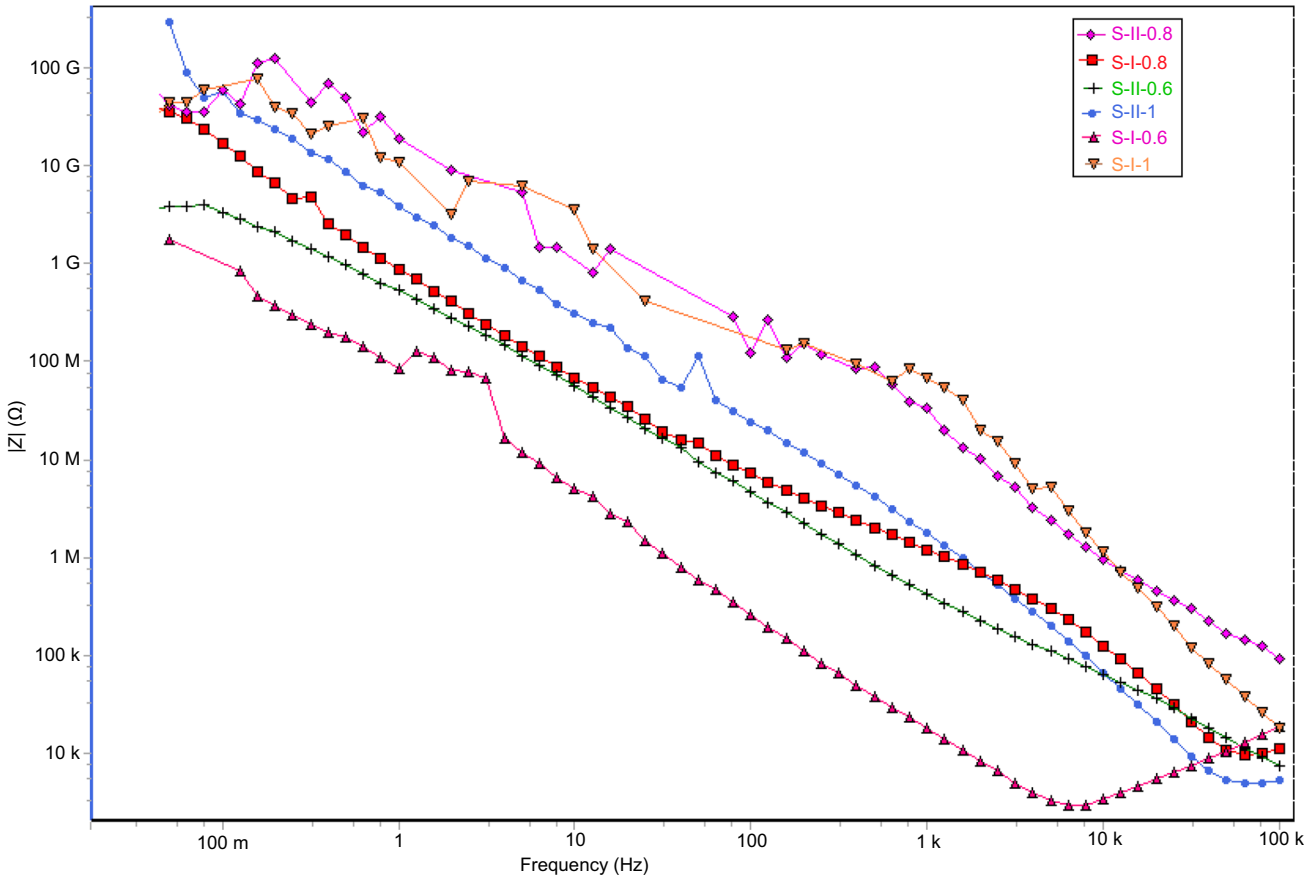

Fig. 6: Bode plots of coatings cured with S-I and S-II

Table 7: Corrosion resistance of coatings cured with S-I and S-II

Coating	Coating resistance
S-I-0.6	1.71E+09
S-I-0.8	1.43E+10
S-I-1.0	2.02E+10
S-II-0.6	6.39E+09
S-II-0.8	9.27E+10
S-II-1.0	2.91E+11

shown in Table 7, coatings cured with S-II exhibited higher corrosion resistance values than those of the coatings cured with S-I. Results revealed that coatings cured with S-II provided more resistance to the electrochemical reactions at the surface, thus exhibiting superior anticorrosive properties. Furthermore, with increase in the concentration of curing agent, the resistance of the coating increases. These curing agents have the ability to be adsorbed onto the metal surface to block the active sites and inhibit corrosion.[37,38] In addition, the high values of impedance could be related to the hard, rigid, and compact structure of epoxy-ester polymer backbone, presence of silicon, and multifunctional nature of curing agents.

TAFEL ANALYSIS: Tafel analysis was carried out to study corrosion parameters of coatings such as corrosion potential, corrosion current, and corrosion rate. Corrosive action of S-I and S-II could be explained on the basis of adsorption. Both the curing agents contain sulfur and oxygen heteroatoms as well as pi-electrons in their structure. These curing agents get adsorbed on the metal surface and form protective layer with the help of heteroatoms and pi-electrons. During the metal-coating interaction, heteroatoms donate the electron charge into the empty *d*-orbitals of the surface metal atoms. Protonation of heteroatoms makes polymer backbone positively charged, whereas due to adsorption of counter ions, metallic surface becomes negatively charged. This results in electrostatic force of attraction between coating and metal surface which form a strong protective layer on the metal surface and improve corrosion resistance.[39–45] Tafel studies were (as shown in Fig. 7) observed to be consistent with the EIS measurement. With increase in concentration of curing agents, corrosion current and corrosion rate of coatings

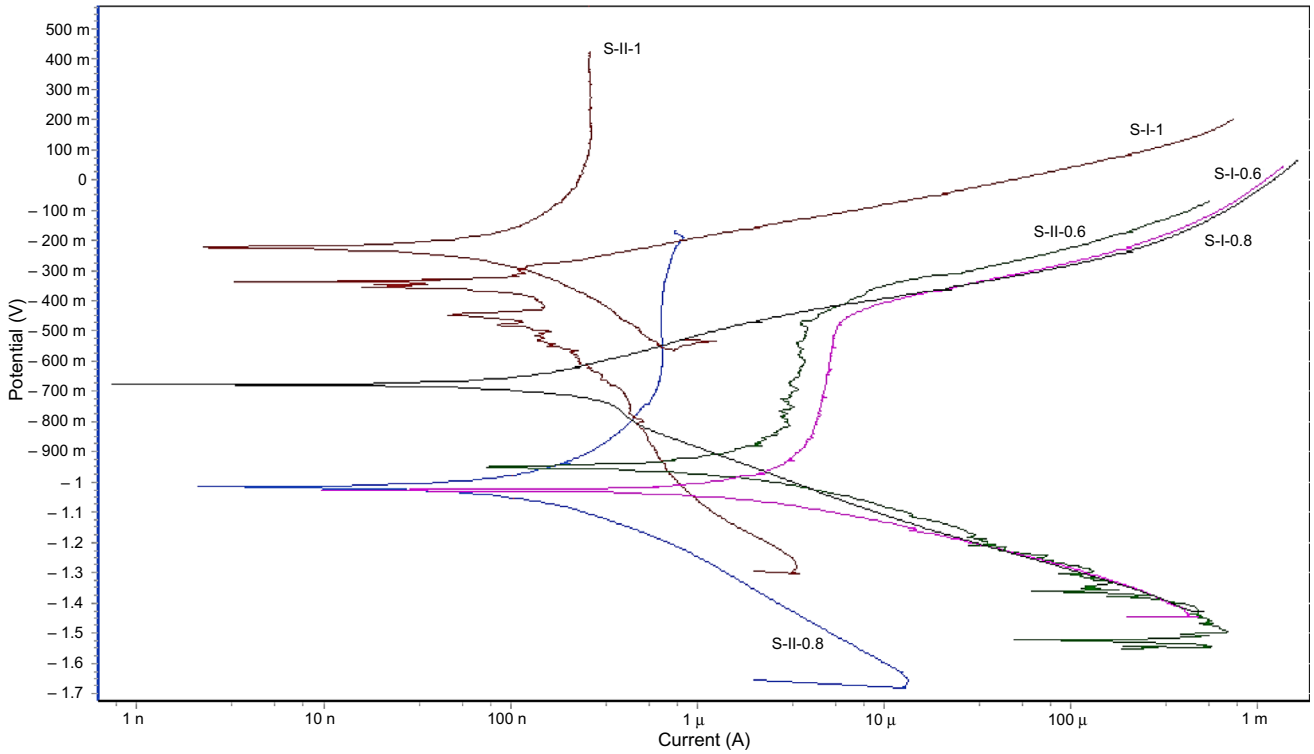

Fig. 7: Tafel plot of coatings cured with S-I and S-II

Table 8: Corrosion parameters of coatings cured with S-I and S-II

Coating	Ecorr (mV)	Icorr (A)	Corrosion rate (mm/yr)
S-I-0.6	– 1025.3	4.5E−06	7.40E−03
S-I-0.8	– 677.2	2.74E−07	4.50E−04
S-I-1.0	– 332.6	1.28E−07	2.10E−04
S-II-0.6	– 953.1	3.2E−06	5.26E−04
S-II-0.8	– 1016.2	9.7E−08	1.60E−04
S-II-1.0	– 224.3	7.47E−08	1.45E−04

were reduced (see Table 8). Moreover, coatings cured with S-II showed slightly lower values of current than that of S-I counterpart. In addition to inhibitive action of S-I and S-II, the presence of hard and compact structure, hydrophobic chains, and silicon atom effectively restricted the flow of electrons through the coating and improved barrier properties of the coatings. As can be seen from corrosion rate values, it was concluded that coatings cured with S-I and S-II showed good anticorrosive properties.

Thermogravimetric analysis (TGA)

Thermogravimetric analysis was carried out to study the degradation behavior of coating films (as shown in Fig. 8). As shown in Table 9, with increase in concentration, initial decomposition temperatures of all the coatings increased. It was also observed that initial decomposition temperatures of coatings cured with S-II were higher than those based on S-I. In addition, irrespective of concentration of curing agent, no significant variation in onset temperature of coatings was observed. However, slight improvement in offset temperature was likely to be seen due to the presence of silicon moiety in the structure. The enhancement in thermal stability could be attributed to the concentration of silicon atom as well as multifunctional nature of curing agents that resulted in hard and compact polymer backbone.

Consequently, % char layer of coatings increased with an increase in concentration of curing agents. It was observed that thermal stability and char yield of coatings cured with S-II were comparatively higher than those of coatings cured with S-I.

Flame retardant properties

Flame retardant properties of all the coatings were evaluated by limiting oxygen index (LOI) and UL-94 tests. Flame retardant properties mainly depend on the amount of silicon–sulfur, functionality of curing agents, and polymer backbone structure. It was observed that only marginal improvement in LOI of the coatings was observed even when high concentration of silicon as well as sulfur was used. As shown in Table 10, for a particular formulation, although silicon content of S-I

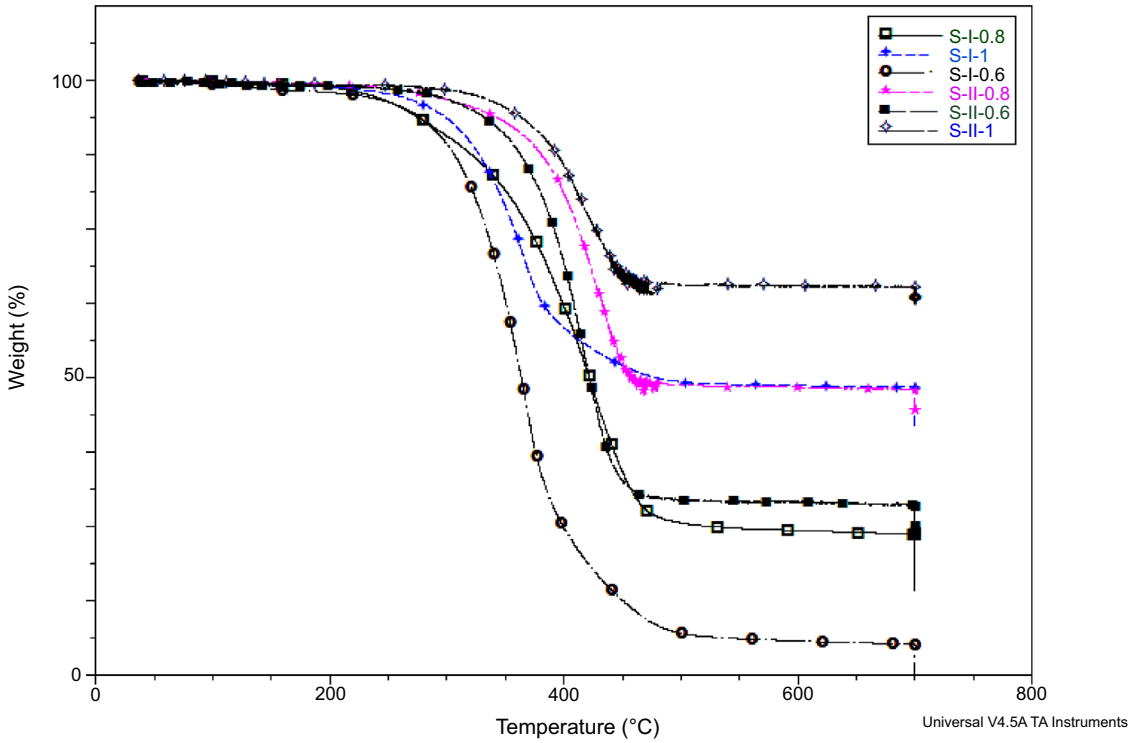

Fig. 8: TGA curves of coatings cured with S-I and S-II

Table 9: TGA values of coatings cured with S-I and S-II

Coating	$T_{5\%}$ (°C)	T_{onset} (°C)	T_{offset} (°C)	Char yield (%)
S-I-0.6	240	305	399	5.74
S-I-0.8	243	313	429	24.8
S-I-1.0	267	309	403	48.2
S-II-0.6	297	351	443	29.2
S-II-0.8	300	363	450	47.3
S-II-1.0	335	365	453	63.1

Table 10: Flame retardant properties of coatings cured with S-I and S-II

Formulation	Limiting oxygen index	UL-94
S-I-0.6	19	VTM-2
S-I-0.8	19	VTM-2
S-I-1.0	20	VTM-1
S-II-0.6	19	VTM-2
S-II-0.8	20	VTM-2
S-II-1.0	21	VTM-1

is higher than that of S-II, no significant improvement was observed in LOI values. On the contrary, coatings cured with S-II showed the highest LOI value of 21. In a similar manner, UL-94 tests showed that flame retardant properties improved with an increase in crosslink density and concentration of silicon and sulfur but could not achieve VTM-0 rating. Moreover, irrespective of concentration of flame retardants, dripping of flammable particles was observed during the UL-94 tests. Overall, it can be concluded that the presence of silicon–sulfur marginally improved flame retardant properties of the coatings.

Biobased content

As per ASTM D6866-05, the biobased content of a product is the amount of biobased carbon in a product as a percent of the weight of the total organic carbon in the product. The biobased content of epoxy-carboxyl curing system could be estimated from the above definition. Products SIL, S-I, and S-II were obtained from the reaction of dichlorodimethylsilane (18.6%

carbon), cardanol (84.56% carbon), and thioglycolic acid (26% carbon). As per reaction stoichiometry, SIL contained 95.45% biobased carbon and accordingly S-I and S-II had 89.26% and 80.60% of biobased carbon content. Based on this, biobased content for all the coating systems could also be evaluated, and it was observed that typical biobased content of epoxy (74.11% carbon)/S-I (89.26% carbon)/*N*,*N*-dimethylbenzene (79.33% carbon) systems ranged from 62.4 to 73.2%. Similarly for coatings based on S-II (80.60% carbon), biobased content ranged from 47.8 to 60.2%.

Conclusion

Multifunctional carboxyl curing agents containing silicon–sulfur were successfully synthesized via thiol-ene coupling and confirmed with chemical as well as spectroscopic analysis. Di- and tetra-functional curing agents were mixed in various concentrations with conventional epoxy resin and evaluated for the coating properties. It was observed that all the coatings exhibited satisfactory mechanical, chemical, optical, and thermal properties independent of the type and concentration of curing agents. Salt spray test revealed that coatings cured with both the curing agents survived 1000 h of salt spray exposure and exhibited superior corrosion resistance. Electrochemical impedance spectroscopy and Tafel analysis complemented the same fact; however, coatings cured with S-II showed slightly higher impedance values and lower corrosion rates to that of S-I counterpart. Thermogravimetric analysis revealed that coatings cured with S-II showed higher offset temperatures and char yield as compared to the S-I counterpart. The presence of two additional functionalities in S-II might have increased crosslink density and improved thermal stability and other coating properties. In case of flame retardant properties, irrespective of curing agents, only marginal improvement was observed as evidenced by LOI and UL-94 tests. Overall, coatings cured with tetra-functional curing agent were observed to exhibit better performance properties than those cured with difunctional curing agent.

Acknowledgments The authors are grateful to Cardolite Specialty Chemicals, India, for providing NC-700 sample. The authors would also like to express their gratitude to UGC-BSR F.25-1/2014-15 (BSR)/No. F.7-314/2010 (BSR) for funding the project.

References

1. Sharif, A, Gupta, A, Sharmin, P, Alam, M, Pandey, S, ''Synthesis, Characterization and Development of High Performance Siloxane-Modified Epoxy Paints.'' *Prog. Org. Coat.*, **54** 248–255 (2005)
2. Kumar, S, Denchev, Z, ''Development and Characterization of Phosphorus-Containing Siliconized Epoxy Resin Coatings.'' *Prog. Org. Coat.*, **66** 1–7 (2009)
3. Kumar, S, Narayanan, T, ''Thermal Properties of Siliconized Epoxy Interpenetrating Coatings.'' *Prog. Org. Coat.*, **45** 323–330 (2002)
4. Lu, S, Hamerton, I, ''Recent Developments in the Chemistry of Halogen-Free Flame Retardant Polymers.'' *Prog. Polym. Sci.*, **27** 1661–1712 (2002)
5. Ravadits, I, Toth, A, Marosi, G, Marton, A, Szep, A, ''Organosilicon Surface Layer on Polyolefins to Achieve Improved Flame Retardancy Through an Oxygen Barrier Effect.'' *Polym. Degrad. Stabil.*, **74** 419–422 (2001)
6. Mercado, L, Galia, M, Reina, J, ''Silicon-Containing Flame Retardant Epoxy Resins: Synthesis, Characterization and Properties.'' *Polym. Degrad. Stabil.*, **91** 2588–2594 (2006)
7. Kashiwagi, T, Gilman, J, In: Grand, AF, Wilkie, CA (eds.) *Fire Retardancy of Polymeric Materials*. Marcel Dekker, New York (2000)
8. Ye, J, Liang, G, Gu, A, Zhang, Z, Han, J, Yuan, L, ''Novel Phosphorus-Containing Hyperbranched Polysiloxane and Its High Performance Flame Retardant Cyanate Ester Resins.'' *Polym. Degrad. Stabil.*, **98** 597–608 (2013)
9. Bajpai, P, Bajpai, M, ''Development of a High Performance Hybrid Epoxy Silicone Resin for Coatings.'' *Pigment Resin Technol.*, **39** 96–100 (2010)
10. Shia, Y, Wang, G, ''The Novel Silicon-Containing Epoxy/PEPA Phosphate Flame Retardant for Transparent Intumescent Fire Resistant Coating.'' *Appl. Surf. Sci.*, **385** 453–463 (2016)
11. Jiang, Y, Li, X, Yang, R, ''Polycarbonate Composites Flame-Retarded by Polyphenylsilsesquioxane of Ladder Structure.'' *J. Appl. Polym. Sci.*, **124** 4381–4388 (2012)
12. Li, L, Li, X, Yang, R, ''Mechanical, Thermal Properties, and Flame Retardancy of PC/Ultrafine Octaphenyl-POSS Composites.'' *J. Appl. Polym. Sci.*, **124** 3807–3814 (2012)
13. Masatoshi, I, Shin, S, ''Silicone Derivatives as New Flame Retardants for Aromatic Thermoplastics Used in Electronic Devices.'' *Polym. Adv. Technol.*, **9** 593–600 (1998)
14. Wang, W, Perng, L, Hsiue, G, Chang, F, ''Characterization and Properties of New Silicone-Containing Epoxy Resin.'' *Polymer*, **41** 6113–6122 (2000)
15. Wu, C, Liu, Y, Chiu, Y, ''Epoxy Resins Possessing Flame Retardant Elements from Silicon Incorporated Epoxy Compounds Cured with Phosphorus or Nitrogen Containing Curing Agents.'' *Polymer*, **43** 4277–4284 (2002)
16. Ding, J, Tao, Z, Zuo, X, Fan, L, Yang, S, ''Preparation and Properties of Halogen-Free Flame Retardant Epoxy Resins with Phosphorus-Containing Siloxanes.'' *Polym. Bull.*, **62** 829–841 (2009)
17. Chen, X, Hu, Y, Jiao, C, Song, L, ''Preparation and Thermal Properties of a Novel Flame-Retardant Coating.'' *Polym. Degrad. Stabil.*, **92** 1141–1150 (2007)
18. Liu, Y, Wu, C, Chiu, Y, Ho, W, ''Preparation, Thermal Properties, and Flame Retardance of Epoxy–Silica Hybrid Resins.'' *J. Polym. Sci. Part A Polym. Chem.*, **41** 2354–2367 (2003)
19. Agrawal, S, Narula, A, ''Synthesis and Characterization of Phosphorus and Silicon Containing Flame-Retardant Curing Agents and a Study of Their Effect on Thermal Properties of Epoxy Resins.'' *J. Coat. Technol. Res.*, **11** 631–637 (2014)
20. Chao, P, Li, Y, Gu, X, Han, D, Jia, X, Wang, M, Zhou, T, Wang, T, ''Novel Phosphorus–Nitrogen–Silicon Flame

Retardants and Their Application in Cycloaliphatic Epoxy Systems.'' *Polym. Chem.*, **6** 2977–2985 (2015)
21. Zhang, L, Wang, Y, Liu, Q, Cai, X, ''Synergistic Effects Between Silicon-Containing Flame Retardant and DOPO on Flame Retardancy of Epoxy Resins.'' *J. Therm. Anal. Calorim.*, **123** 1343–1350 (2016)
22. Feng, Y, He, C, Wen, Y, Ye, Y, Zhou, X, Xie, X, Mai, Y, ''Improving Thermal and Flame Retardant Properties of Epoxy Resin by Functionalized Graphene Containing Phosphorous, Nitrogen and Silicon Elements.'' *Compos. Part A*, **103** 74–83 (2017)
23. Balgude, D, Konge, K, Sabnis, A, ''Synthesis and Characterization of Sol–Gel Derived CNSL Based Hybrid Anti-Corrosive Coatings.'' *J. Sol–Gel Sci. Technol.*, **69** 155–165 (2014)
24. Kathalewar, M, Sabnis, A, D'Mello, D, ''Isocyanate Free Polyurethanes from New CNSL Based Bis-Cyclic Carbonate and Its Application in Coatings.'' *Eur. Polym. J.*, **57** 99–108 (2015)
25. Wazarkar, K, Sabnis, A, ''Development of Cardanol Based Polyol via Click Chemistry and Crosslinking with Melamine Formaldehyde Resin for Coating Applications.'' *J. Renew. Mater.*, **5** 3–4 (2017)
26. Balgude, D, Sabnis, A, Ghosh, S, ''Designing of Cardanol Based Polyol and Its Curing Kinetics with Melamine Formaldehyde Resin.'' *Des. Monomers Polym.*, **20** 177–189 (2017)
27. Wazarkar, K, Kathalewar, M, Sabnis, A, ''High Performance Polyurea Coatings Based on Cardanol.'' *Prog. Org. Coat.*, **106** 96–110 (2017)
28. Balgude, D, Sabnis, A, Ghosh, S, ''Synthesis and Characterization of Cardanol Based Reactive Polyamide for Epoxy Coating Application.'' *Prog. Org. Coat.*, **104** 250–262 (2017)
29. Xiong, Z, Ma, S, Fan, L, Tang, Z, Zhang, R, Na, H, Zhu, J, ''Surface Hydrophobic Modification of Starch with Bio-Based Epoxy Resins to Fabricate High-Performance Polylactide Composite Materials.'' *Compos. Sci. Technol.*, **94** 16–22 (2014)
30. Voirin, C, Caillol, S, Sadavarte, N, Tawade, B, Boutevin, B, Wadgaonkar, P, ''Functionalization of Cardanol: Towards Bio-Based Polymers and Additives.'' *Polym. Chem.*, **5** 3142–3162 (2014)
31. Wazarkar, K, Kathalewar, M, Sabnis, A, ''Anticorrosive and Insulating Properties of Cardanol Based Anhydride Curing Agent for Epoxy Coatings.'' *React. Funct. Polym.*, **122** 148–157 (2018)
32. Bentiss, F, Lebrini, M, Lagrenee, M, ''Thermodynamic Characterization of Metal Dissolution and Inhibitor Adsorption Processes in Mild Steel/2,5-Bis(*n*-Thienyl)-1,3,4-Thiadiazoles/Hydrochloric Acid System.'' *Corros. Sci.*, **47** 2915–2931 (2005)
33. Popova, A, Christov, M, Zwetanova, A, ''Effect of the Molecular Structure on the Inhibitor Properties of Azoles on Mild Steel Corrosion in 1 M Hydrochloric Acid.'' *Corros. Sci.*, **49** 2131–2143 (2007)
34. Bharara, K, Kim, H, Singh, G, ''Inhibiting Effects of Butyl Triphenyl Phosphonium Bromide on Corrosion of Mild Steel in 0.5 M Sulphuric Acid Solution and Its Adsorption Characteristics.'' *Corros. Sci.*, **50** 2747–2754 (2008)
35. Ahmed, S, Ali, W, Khadom, A, ''Synthesis and Investigations of Heterocyclic Compounds as Corrosion Inhibitors for Mild Steel in Hydrochloric Acid.'' *Int. J. Ind. Chem.*, **10** 159–173 (2019)
36. Kumar, S, Sasikumar, A, ''Studies on Novel Silicone/Phosphorus/Sulphur Containing Nano-Hybrid Epoxy Anticorrosive and Antifouling Coatings.'' *Prog. Org. Coat.*, **68** 189–200 (2010)
37. Jafari, H, Danaee, I, Eskandari, H, Rashvandavei, M, ''Electrochemical and Theoretical Studies of Adsorption and Corrosion Inhibition of N,N′-Bis(2-Hydroxyethoxyacetophenone)-2,2-Dimethyl-1,2-Propanediimine on Low Carbon Steel (API 5L Grade B) in Acidic Solution.'' *Ind. Eng. Chem. Res.*, **52** 6617–6632 (2013)
38. Jafari, H, Sayin, K, ''Sulphur Containing Compounds as Corrosion Inhibitors for Mild Steel in Hydrochloric Acid Solution.'' *Trans. Indian Inst. Met.*, **69** 805–815 (2016)
39. Quraishi, M, Sardar, R, ''Effect of Some Nitrogen And Sulphur Based Synthetic Inhibitors on Corrosion Inhibition of Mild Steel in Acid Solutions.'' *Indian J. Chem. Technol.*, **11** 103–107 (2004)
40. Khaled, K, Al-Qahtani, M, ''The Inhibitive Effect of Some Tetrazole Derivatives Towards Al Corrosion in Acid Solution: Chemical, Electrochemical and Theoretical Studies.'' *Mater. Chem. Phys.*, **113** 150–158 (2009)
41. Oguzie, E, Li, Y, Wang, F, ''Corrosion Inhibition and Adsorption Behaviour of Methionine on Mild Steel in Sulphuric Acid and Synergistic Effect of Iodide Ion.'' *J. Colloid Interface Sci.*, **310** 90–98 (2007)
42. Sherif, E, Park, S, ''2-Amino-5-Ethyl-1,3,4-Thiadiazole as a Corrosion Inhibitor for Copper in 3.0% NaCl Solutions.'' *Corros. Sci.*, **48** 4065–4079 (2006)
43. Tabatabaei, F, Sarabi, A, Kowsari, E, Mohammadloo, H, ''Electrochemical and Morphological Study of Steel in 1 M HCl in the Presence of Task Specific Liquid.'' *J. Mater. Eng. Perform.*, **24** 3433–3443 (2015)
44. Ituen, E, Essien, E, Udo, U, Oluwaseyi, O, ''Experimental and Theoretical Study of Corrosion Inhibition Effect of *Cucumeropsis mannii* N. Seed Oil Metallic Soap of Zinc on Mild Steel Surface in Sulphuric Acid.'' *Adv. Appl. Sci. Res.*, **5** 26–53 (2014)
45. Verma, C, Verma, D, Ebenso, E, Quraishi, M, ''Sulphur and Phosphorus Heteroatom Containing Compounds as Corrosion Inhibitors: An Overview.'' *Heteroatom Chem.*, **29** e21437 (2018)